ARTICLES

Self-assembly Synthesis of Single-Crystalline Tin Oxide Nanostructures by a Poly(acrylic acid)-Assisted Solvothermal Process

Guoe Cheng,[†] Jinmin Wang,[†] Xiangwen Liu,[‡] and Kaixun Huang*,[†]

Department of Chemistry, Huazhong University of Science and Technology, Wuhan 430074, P.R. China, and State Key Laboratory of Geological Process and Mineral Resources, China University of Geosciences, Wuhan 430074, P.R. China

Received: March 29, 2006; In Final Form: May 12, 2006

Single-crystalline SnO_2 nanocones with an average 1.0 μm in length and 100−500 nm in root size and their self-assembly morphologies were obtained through a solvothermal process in the presence of poly(acrylic acid). X-ray diffraction, electron microscopy, Raman scattering spectra, and infrared (IR) spectra were used to characterize the nanocones. The as-synthesized SnO_2 nanocones with the typical rutile phase exhibit preferential growth along the [001] direction and high chemical stability. The proposed mechanism for the formation of SnO_2 nanocones and the further self-assembly into hollow sphere-like superstructure is discussed.

1. Introduction

Morphological control of nanostructured semiconductors is of great significance for systematic fundamental studies of crystal growth and for exploring new applications of nanostructures due to the interesting size- and shape-dependent properties.[1] Tin oxide (SnO_2) is a stable and n-type wide band gap semiconductor (Eg = 3.6 eV) with excellent optical and electrical properties. It is widely used as transparent electrodes, as gas sensors, in storage applications, and as solar cells.[2] SnO_2 nanoparticles and thin films have been prepared by a variety of techniques, including hydrothermal,[3] sol−gel,[4] solution phase,[5] magnetron sputtering,[6] and so forth. Recently, low-dimensional single-crystalline SnO_2 nanostructures such as nanobelts and nanowires were prepared by thermal evaporation,[7] laser ablation technique,[8] and oxidation of elemental tin.[9] SnO_2 nanotubes were also prepared by template-based methods,[10] but they all were polycrystalline. Solution-based growth is always considered to be of distinct advantage to morphological control of nanocrystals. However, using solution-based routes to prepare nanoscale single-crystalline SnO_2 with tunable dimensions and sizes still remains a great challenge. Only single-crystalline SnO_2 nanorods[11] and polycrystalline SnO_2 nanowires[12] have been obtained in solutions by now.

Recently, nanocones, a new kind of quasi one-dimensional nanostructure with nanometer-sized tips and micrometer-sized bases, have attracted considerable interest because of their potential applications in nanoscaled manipulation, in field emission, and as optical microscopy probes. For example, they can be used as field emitters and in scanning probe microscopy due to their mechanical stiffer, less prone to bending and thermal stability.[13d] However, to date the obtained nanocones are still restricted to a very few members such as carbon, silicon, boron nitride, silicon carbide, zinc oxide, and aluminum nitride due to the difficulty in preparation.[13]

In this article, we report for the first time a facile solution route to synthesize single-crystalline rutile SnO_2 nanocones and their self-assembly superstructures with high chemical stability. The experiments were performed by a solvothermal process assisted by a long-chain polymer poly(acrylic acid) (PAA) in water and water/ethanol media and this process has proved to be readily reproducible.

2. Experimental Section

$SnCl_4 \cdot 5H_2O$ was used as the starting material, sodium hydroxide was used as a mineralizer, and poly(acrylic acid) (PAA, M_w = 800−1000 g mol^{-1}, 30 wt % in water) was used as an additive. All reagent-grade chemicals were used as received without further purification. Distilled water was used for preparing an aqueous $SnCl_4$ solution. In a typical procedure, 1.20 g of sodium hydroxide was added to 60 mL of aqueous solution containing 1.05 g of $SnCl_4 \cdot 5H_2O$ under stirring. When the solution became transparent and $Sn(OH)_6^{2-}$ was formed in the basic solution, 1.67 g of PAA was introduced. After several minutes of stirring, the obtained solution was transferred to a 80 mL stainless steel Teflon-lined autoclave. Solvothermal treatment was performed by placing the autoclave in an oven at 200 °C for 15 h and cooling to room temperature naturally. After ultrasonication for 15 min, the milk white aqueous suspension was collected and washed with distilled water and absolute ethanol for several times. Finally, the products were dried in air at 60 °C for 24 h for further characterization.

The phase structure and phase purity of the as-synthesized powders were examined by X-ray diffraction (XRD, X'pert PRD, Cu Kα radiation with λ = 1.5406 Å). The morphologies and sizes of the products were further observed by field-emission scanning electron microscopy (FESEM, FEI Sirion 200). The

* To whom correspondence should be addressed. E-mail: hxxzrf@mail.hust.edu.cn. Phone: 86-27-87543133. Fax: 86-27-87543632.
[†] Huazhong University of Science and Technology.
[‡] China University of Geosciences.

10.1021/jp061935q CCC: $33.50
Published on Web 08/02/2006

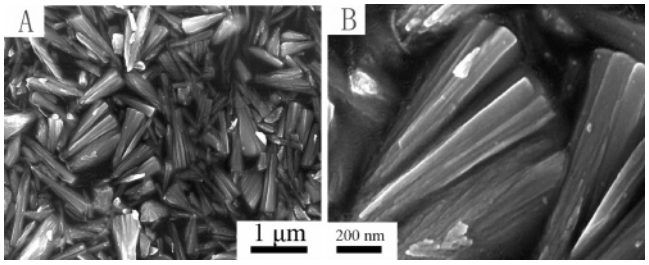

Figure 1. Representative SEM images (A) and high-magnification SEM images (B) of the SnO_2 nanocones prepared in a water medium.

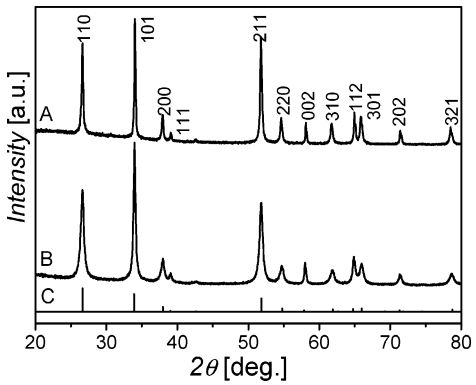

Figure 2. XRD patterns of the synthesized SnO_2 nanocones: (A) prepared in a water medium; (B) prepared in an alcohol/water medium; (C) the standard data from JCPDS file No. 41-1445.

microscopic nanostructures were observed by transmission electron microscopy (TEM, FEI Tecnai G2 20 operated at 200 kV) and high-resolution transmission electron microscopy (HRTEM/SAED, JEM-2010FEF operated at 200 kV). The infrared (IR) spectra were recorded on a Fourier transform infrared (FT-IR) spectrometer (EQUINOX Bruker) using KBr pellet technique in the spectra range of 4000−400 cm^{-1}. Raman scattering spectra were measured with a Renishaw/invia Raman microscope at room temperature. The 514 nm line of an Ar^+ laser was used for the excitation source.

3. Results and Discussion

Low-magnification SEM observation (Figure 1A) shows that the obtained SnO_2 crystallites exhibit a well-defined conelike morphology with an average 1.0 μm in length and 100−500 nm in size at their bases. The magnified FESEM image in Figure 1B clearly reveals that the cross section of these conelike nanostructures is not in round form but in irregular and elongated shapes. It also can be seen that the nanocones possess rugged surfaces with some grooves which dramatically increase the surface area.

The XRD pattern of these nanocones is shown in Figure 2A. All the diffraction peaks can be well-indexed to the rutile structure of SnO_2 with tetragonal lattice parameters $a = 4.737$ Å and $c = 3.172$ Å, which belong to the space group of $P4_2/mnm$ according to the JCPDS file No. 41-1445. No other crystallographic phase can be detected. However, it is obviously found that the relative intensity of the peaks deviates from that of the bulk material, indicating the anisotropic growth of the SnO_2 crystals.

Figure 3A gives a typical TEM image of an isolated nanocone and a selected area electron diffraction pattern (SAED) (inset), indicating that the as-prepared nanocones are single-crystalline with the [001] axial direction as illustrated in the inset of Figure 3A. The HRTEM image (Figure 3B) observed at the tip part and the corresponding Fourier transform pattern (FFT) (Figure 3B, inset) further confirm the single-crystal nature of the nanocones. The spacing between adjacent lattice planes is 0.263 nm, corresponding to (101) planes of rutile SnO_2. Combined with the results of FFT analysis, the preferential growth direction is [001].

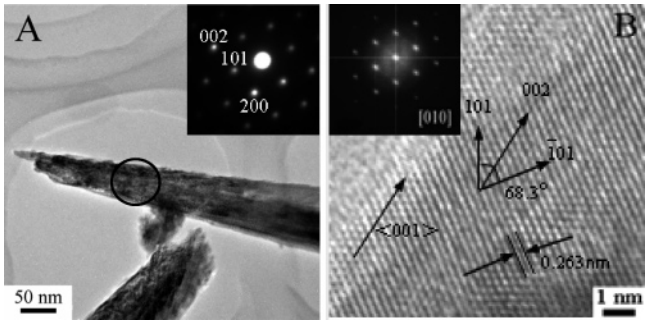

Figure 3. Typical TEM and high-resolution TEM (HRTEM) images of the SnO_2 nanocones prepared in a water medium. (A) TEM image of an individual SnO_2 nanocone (inset, a selected area electron diffraction pattern); (B) HRTEM image of the SnO_2 nanocone at its tip section (inset, corresponding Fourier transform pattern).

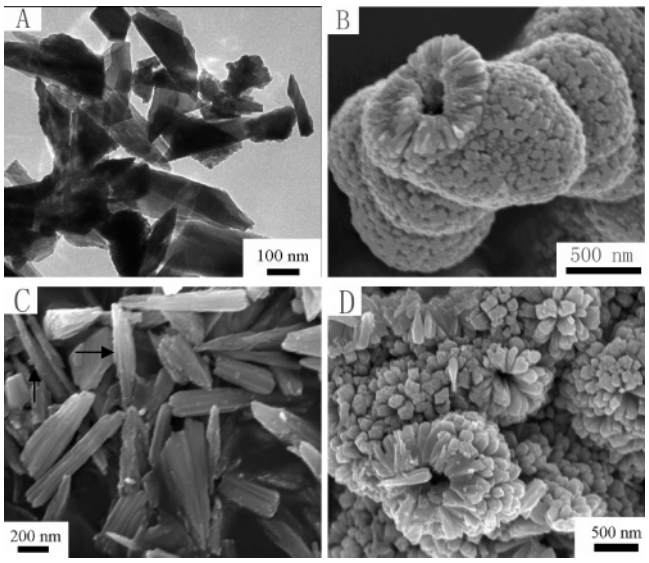

Figure 4. (A) Typical TEM image of the SnO_2 prepared in a water medium without introduction of PAA; (B) representative SEM image of SnO_2 nanocone-based assemblies when the dosage of PAA was up to 5.0 g in a water medium; (C) and (D) representative SEM images of SnO_2 nanocrstallites and the hollow spherelike assemblies prepared in an alcohol/water medium.

The water-soluble long-chain additive PAA was proved to play an important role in the space-limited growth of SnO_2 crystallite and subsequent self-assembly process. Control experiments have shown that, without PAA, many irregular SnO_2 structures were obtained (Figure 4A); with an increase in the dosage of PAA up to 5.0 g, hollow spherelike superstructures with many gaps existing inside the superstructures are observed, indicating these superstructures are built from nanocone subunits. However, no individual nanocones existed in our samples (Figure 4B); on the other hand, when the experiment was performed in an alcohol−water medium (1:2, v/v), a changed morphology is observed. Besides the typical nanocones observed in the products prepared in water, some slender nanocones and nanorods with the diameter less than 100 nm (indicated by arrows) and many quasi-nanocone structures without sharp tips are formed (Figure 4C). Those irregular nanostructures form incompact hollow spherelike clusters (Figure 4D). Its XRD

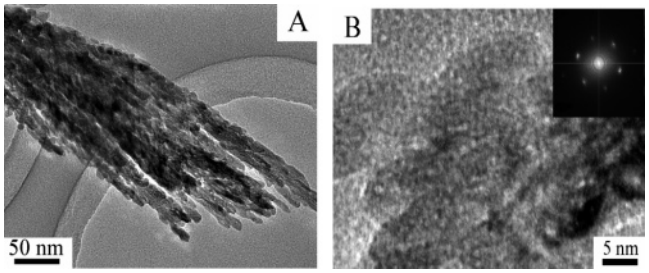

Figure 5. Typical TEM (A) and high-resolution TEM (HRTEM) (B) images of the aggregation morphologies of SnO_2 nanoparticles prepared in water media (inset, corresponding Fourier transform pattern (FFT)).

pattern (Figure 2B) also reveals the anisotropic growth of the rutile SnO_2 crystallites.

It is believed that the long-chain PAA may direct the aggregation of colloidal particles and subsequent crystallization. The whole growth process of the SnO_2 nanostructures can be described as a self-assembly and oriented attachment mechanism. In the initial stage of the solvothermal reaction, the complex $Sn(OH)_6^{2-}$ decomposed quickly and a massive SnO_2 nuclei were created, resulting in immediate solution supersaturation due to the low solubility of SnO_2. These SnO_2 nuclei spontaneously cluster together to minimize their surface area and nanoparticles were formed in the colloidal solution. At the same time, with the strong interactions between the SnO_2 crystallites and the active side group ions COO^- in the PAA, some surfaces of the growth units are modified by the complex ions. This combination makes these nanoparticles building blocks that attach to the surroundings of the PAA long chain and further assemble into conelike aggregates. According to Banfield et al.,[14] jiggling of nanoparticles by Brownian motion may allow adjacent particles to rotate to find the low-energy configuration represented by a coherent particle−particle interface. For the rutile structure of SnO_2, the surface energy per crystal face forms the sequence (110) < (100) < (101) < (001) according to the calculated data.[15] The nanoparticles would at first rotate to align along the [001] direction and form chainlike structures, which would further aggregate into clusters to minimize the surface energy. Figure 5 shows the earlier morphologies of this aggregation from which we can clearly observe that quasi-spherical nanoparticles with the size of 5−15 nm are interconnected along a common crystallographic axis and assembled into tufts, like paddies. When these particles become almost perfectly aligned, the particles are epitaxially syncretized together under the high-pressure and high-temperature conditions and continuous single crystals are formed. The crystal growth process is accomplished by eliminating PAA at the interfaces. FT-IR spectra (not shown) of the products reveal that the surfaces of obtained SnO_2 nanocones are still adsorbed by a small amount of polymer. Oriented aggregation was most commonly detected in colloids. Cheng et al.[11b] and Chen and Gao[11c] have also reported *c*-elongated anisotropic growth by the solvothermal process using water/ethanol as the reaction media, but the sizes of the obtained nanorods are relatively small. According to Vayssieres and Graetzel,[11d] the centrosymmetric structure of low-axial ratios ($c/a = 0.67$) reduces substantially the possibility of anisotropic growth of the crystals along the [001] direction. However, in this experiment, we obtained single-crystalline nanocones with larger dimensions in both water and water/ethanol media. In the alcohol−water media, we also observed the conelike aggregation morphologies of the nanoparticles. However, a slow nucleation in the initial stage and existing morphologies of PAA long chains changed

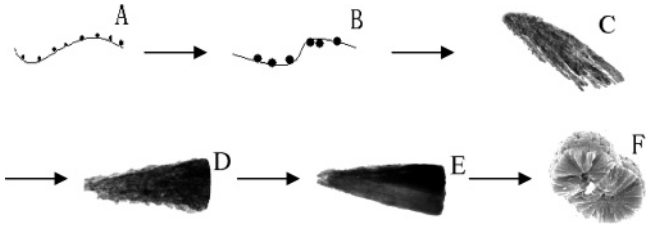

Figure 6. Schematic illustration of the proposed mechanism for the formation of SnO_2 nanocones and further self-assembly into hollow spherelike superstructures. (A) SnO_2 nuclei absorbed by PAA in the colloid solution; (B) formation of the secondary quasi-spherical nanoparticles; (C) aggregation of the secondary quasi-spherical nanoparticles directed by PAA; (D) formation of the nanocones by the quasi-spherical nanoparticles; (E) single-crystalline SnO_2 nanocones were obtained; (F) the self-assembly of the SnO_2 nanocones into hollow sphere-like superstructures.

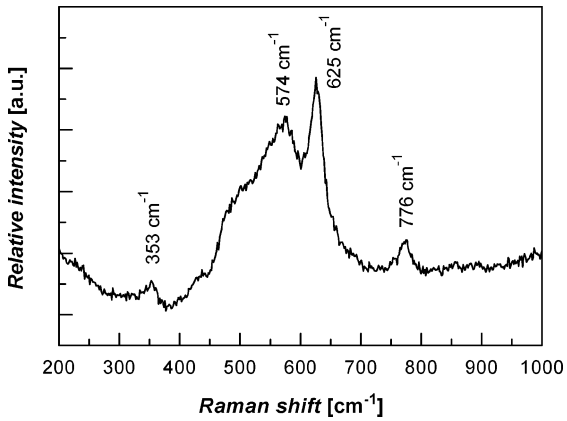

Figure 7. Room-temperature Raman spectrum of the as-prepared SnO_2 nanocones.

due to the insolubility of PAA in alcohol, resulting in the formation of different nanostructures.

With a large amount of gaps existing in the superstructures, the as-obtained hollow spherelike self-assemblies are very stable and could not be destroyed and broken into individual nanocones after 15 min of ultrasonication. Since weak van der Waals' forces between the nanocones are not enough to stabilize these superstructures,[16] the strong chemical bonding is thus believed to be formed to integrate lateral surfaces during the self-assembly. The PAA has proved to be a template for the formation of the hollow spherelike superstructures. At the same time, with nanometer-sized tips and rugged surfaces, the nanocones have high surface free energy, which make it easy to further assemble into hierarchical structures. For example, when the lateral surfaces of these tips share a common crystallographic orientation, bonding between the tips were created to reduce overall energy. The whole formation process is illustrated in Figure 6.

Figure 7 shows the room-temperature Raman spectrum of the as-synthesized SnO_2 nanocones. Two normal phonon modes, A_{1g} and B_{2g}, which are related to the expansion and contraction vibration mode of Sn−O bonds and usually appear in bulk single crystals or polycrystalline SnO_2 materials, are detected at 625 and 776 cm^{-1}, respectively. These Raman features further confirm that the as-synthesized SnO_2 nanocones possess the features of the tetragonal rutile structure. In addition to these classical vibration modes, two additional Raman scattering peaks at 574 and 353 cm^{-1}, which are not found in Raman spectra of bulk SnO_2 crystals, can be observed in these SnO_2 nanocones. This phenomenon is believed to be related to the microstructure of components of SnO_2 nanocrystallites. The defects of nano-

crystals such as vacancies of oxygen, vacancy clusters, and local lattice disorder at the interface and interior surface will lead to a significant lattice distortion and an evident space-symmetry reduction of D_{4h}^{14} and the appearance of a group of new Raman peaks. The vibration mode of the two peaks agrees very well with the Matossi force constant model.[17a] Similar shift peaks have been reported in the case of SnO_2 nanorods[11b] and nanoparticles.[17]

The SnO_2 nanostructures with rutile phase are of high chemical stability. The corrosion resistance of the as-prepared SnO_2 in aqueous solution of acids and bases indicated that the SnO_2 powders are insoluble in many kinds of acids or bases, even at high temperature. This property is expected to be useful for the applications of SnO_2 advanced devices.

4. Conclusion

In summary, single-crystalline SnO_2 nanocones with an average 1.0 μm in length and 100−500 nm in root size and their self-assembly morphologies were obtained through a facile solvothermal process in the presence of PAA. XRD patterns, room-temperature Raman spectrum, and HRTEM images show that the as-prepared SnO_2 nanocones are of a crystalline rutile structure and exhibit preferential growth along the [001] direction. The crystal growth experienced a self-assembly and oriented attachment process and the existence of PAA has been found to be a soft template for the growth of SnO_2 nanocones. Furthermore, the nanometer-sized tips and rugged surfaces of the SnO_2 nanocones resulted in the further self-assembly into hollow spherelike superstructures. Due to high chemical stability in acid and alkaline solutions, accompanied by the unique properties of the nanocones, we expect to explore the new application of the SnO_2 nanocones. Moreover, it is believed that this synthetic process of the SnO_2 nanocones can be used to prepare other single-crystalline nanostructures or be a good reference to design and prepare single-crystalline SnO_2 with other morphologies.

Acknowledgment. We thank the faculty from the Analytical and Testing Center of Huazhong University of Science and Technology and Mr. Dongshan Zhao from Wuhan University for technical assistance on characterizations.

References and Notes

(1) Burda, C.; Chen, X.; Narayanan, R.; El-Sayed, M. A. *Chem. Rev.* **2005**, *105*, 1025.

(2) (a) Elangovan, E.; Ramamurthi, K.; Optoelectron, J. *Adv. Mater.* **2003**, *5*, 45. (b) Law, M.; Kind, H.; Messer, B.; Kim, F.; Yang, P. D. *Angew. Chem., Int. Ed.* **2002**, *41*, 2405. (c) Park, N.; Kang, M. G.; Ryu, K. S.; Kim, K. M.; Chang, S. H. *J. Photochem. Photobiol. A* **2004**, *161*, 105. (d) Ferrere, S.; Zaban, A.; Gregg, B. A. *J. Phys. Chem. B* **1997**, *101*, 4490.

(3) Fujihara, S.; Maeda, T.; Ohgi, H.; Hosono, E.; Imai, H.; Kim, S. H. *Langmuir* **2004**, *20*, 6476.

(4) (a) Pang, G.; Chen, S.; Koltypin, Y.; Zaban, A.; Feng, S.; Gedanken, A. *Nano Lett.* **2001**, *1*, 723. (b) Leen, S. C.; Lee, J. H.; Oh, T. S.; Kim, Y. H. *Sol. Energy Mater. Sol. Cells* **2003**, *75*, 481.

(5) (a) Jiang, L.; Sun, G.; Zhou, Z.; Sun, S.; Wang, Q.; Yan, S.; Li, H.; Tian, J.; Guo, J.; Zhou, B.; Xin, Q. *J. Phys. Chem. B* **2005**, *109*, 8744. (b) Ohgi, H.; Maeda, T.; Hosono, E.; Fujihara, S.; Imai, H. *Cryst. Growth Des.* **2005**, *5*, 1079.

(6) Karapatnitski, I. A.; Mit', K. A.; Mukhamedshina, D. M.; Beisenkhanov, N. B. *Surf. Coat. Technol.* **2002**, *151*−*152*, 76.

(7) (a) Pan, Z. W.; Dai, Z. R.; Wang, Z. L. *Science* **2001**, *291*, 1947. (b) Dai, Z. R.; Pan, Z. W.; Wang, Z. L. *J. Phys. Chem. B* **2002**, *106*, 1274. (c) Chen, Y.; Cui, X.; Zhang, K.; Pan, D.; Zhang, S.; Wang, B.; Hou, J. G. *Chem. Phys. Lett.* **2003**, *369*, 16.

(8) (a) Hu, J.; Bando, Y.; Liu, Q.; Golberg, D. *Adv. Funct. Mater.* **2003**, *13*, 493. (b) Liu, Z. Q.; Zhang, D. H.; Han, S.; Li, C.; Tang, T.; Jin, W.; Liu, X. L.; Lei, B.; Zhou, C. W. *Adv. Mater.* **2003**, *15*, 1754.

(9) (a) Duan, J.; Yang, S.; Liu, H.; Gong, J.; Huang, H.; Zhao, X.; Zhang, R.; Du, Y. *J. Am. Chem. Soc.* **2005**, *127*, 6180. (b) Hu, J. Q.; Ma, X. L.; Shang, N. G.; Xie, Z. Y.; Wong, N. B.; Lee, C. S.; Lee, S. T. *J. Phys. Chem. B* **2002**, *106*, 3823.

(10) (a) Wang, Y.; Lee, J. Y.; Zeng, H. C. *Chem. Mater.* **2005**, *17*, 3899. (b) Huang, J.; Matsunaga, N.; Shimanoe, K.; Yamazoe, N.; Kunitake, T. *Chem. Mater.* **2005**, *17*, 3513.

(11) (a) Zhang, D. F.; Sun, L. D.; Yin, J. L.; Yan, C. H. *Adv. Mater.* **2003**, *15*, 1022. (b) Cheng, B.; Russe, J. M.; Shi, W.; Zhang, L.; Samulski, E. T. *J. Am. Chem. Soc.* **2004**, *126*, 5972. (c) Chen, D.; Gao, L. *Chem. Phys. Lett.* **2004**, *398*, 201. (d) Vayssieres, L.; Graetzel, M. *Angew. Chem., Int. Ed.* **2004**, *43*, 3666.

(12) Wang, Y.; Jiang, X.; Xia, Y. *J. Am. Chem. Soc.* **2003**, *125*, 16176.

(13) (a) Zhang, G. Y.; Jiang, X.; Wang, E. G. *Science* **2003**, *300*, 472. (b) Cao, L.; Laim, L.; Ni, C.; Nabet, B.; Spanier, J. E. *J. Am. Chem. Soc.* **2005**, *127*, 13782. (c) Azevedo, S.; Mazzoni, M. S. C.; Chacham, H.; Nunes, R. W. *Appl. Phys. Lett.* **2003**, *82*, 2323. (d) Lin, M.; Loh, K. P.; Boothroyd, C.; Du, A. Y. *Appl. Phys. Lett.* **2004**, *85*, 5388. (e) Han, X.; Wang, G.; Jie, J.; Choy, W. C. H.; Luo, Y.; Yuk, T. I.; Hou, J. G. *J. Phys. Chem. B* **2005**, *109*, 2733. (f) Liu, C.; Hu, Z.; Wu, Q.; Wang, X. Z.; Chen, Y.; Sang, H.; Zhu, J. M.; Deng, S. Z.; Xu, N. S. *J. Am. Chem. Soc.* **2005**, *127*, 1318.

(14) Banfield, J. F.; Welch, S. A.; Zhang, H.; Ebert, T. T.; Penn, R. L. *Science* **2000**, *289*, 751.

(15) Leite, E. R.; Giraldi, T. R.; Pontes, F. M.; Longo, E.; Beltran, A.; Andres, J. *Appl. Phys. Lett.* **2003**, *83*, 1566.

(16) Korgel, B. A.; Fitzmaurice, D. *Adv. Mater.* **1998**, *10*, 661.

(17) (a) Yu, K. N.; Xiong, Y. H.; Liu, Y. L.; Xiong, C. S. *Phys. Rev. B* **1997**, *55*, 2666. (b) Zuo, J.; Xu, C.; Liu, X.; Wang, C.; Wang. C.; Hu, Y.; Qian, Y. *J. Appl. Phys.* **1994**, *75*, 1835.